Stochastic Ex-Ante LCA under Multidimensional Uncertainty

Anticipating the Production of Undiscovered Microalgal Compounds in Europe

Jouannais, Pierre; Pizzol, Massimo

Published in:
Environmental Science and Technology

DOI (link to publication from Publisher):
10.1021/acs.est.2c04849

Publication date:
2022

Document Version
Accepted author manuscript, peer reviewed version

Stochastic Ex-ante LCA Under Multidimensional Uncertainty: Anticipating the Production of Undiscovered Microalgal Compounds in Europe

AUTHOR NAMES

Pierre Jouannais[1]*, Massimo Pizzol**[1]

AUTHOR ADDRESS

[1] Department of Planning, Aalborg University, Rendsburggade 14, 9000 Aalborg, Denmark

*corresponding author

KEYWORDS

Life-Cycle Assessment, Uncertainty, Ex-ante, Microalgae, Industrial Ecology

ABSTRACT

Due to their biodiversity, microalgae represent a promising source of high-value compounds that bioprospecting is aiming to reveal. Performing an ex-ante Life Cycle Assessment (LCA) to anticipate and potentially minimize the environmental burden associated with the European production of a bioprospected microalgal compound is subject to substantial and multi-factorial uncertainty, as the compound remains undiscovered. Given that any microalgal strain could potentially host the compound of interest, the ex-ante LCA should consider this bioprospecting uncertainty together with the uncertainty on the technology and the production mix.

Using a parameterized cultivation simulation and consequential LCA model, and an extensive stochastic pseudo Monte Carlo approach, we define and propagate techno-operational, bioprospecting, and production mix uncertainties for a microalgal compound being currently bioprospected in Europe. We perform global sensitivity analysis using different sampling strategies to identify the main contributors to the total output variance. Overall, the uncertainty propagation allowed us to define and analyze the probabilistic scope for the potential environmental impacts in the emerging production of high-value microalgal compounds in Europe, based on current knowledge. These findings can support policy-making as well as actors in the microalgal sector towards technological paths with lower environmental impact.

SYNOPSIS

We anticipate the environmental impacts associated with the European production of a currently bioprospected microalgal compound via a stochastic, ex-ante, and consequential LCA based on microalgal cultivation simulations.

TEXT

1. Introduction

The biological diversity of microalgae makes them a promising biological group for biotechnological applications such as the production of organic products of high commercial value. Among these products, while microalgae-based 3rd generation biofuels have so far failed to compete economically with fossil fuels[1], a few high-value microalgal compounds are already commercialized[2,3]. Recent discoveries from bioprospecting, i.e. the search for compounds and properties within the biodiversity that could be valuable for human activities, range from antimicrobial to antitumoral lipids, proteins, and carbohydrates in microalgal strains[4–10]. This suggests that the European microalgae sector might develop substantially in the near future. Anticipating the environmental consequences of such a development is crucial as early-stage emerging systems are characterized by a high design freedom[11] implying potential detrimental scenarios and because sustainable development processes *"are timely, anticipatory, integrative, flexible and action focused"*[12]. Life Cycle Assessment (LCA) constitutes a robust holistic tool to quantitatively anticipate such impacts on a systemic level and offers flexibility and parametrization to project different scenarios.

LCA studies on the environmental impacts of microalgae production address primarily bioenergy-oriented microalgae growth in Open Pond Raceways[13–18], while high-value compounds production would likely require stable and contamination-free photobioreactors (PBR). When reviewing eighteen existing LCA studies of microalgae[19–27], we found that they consider only seven well-studied strains. This is likely because the microalgal sector has historically focused on bioenergy applications and therefore primary data and assumptions on yields and operating

63 conditions exist only for a restricted set of strains that are fit for bioenergy and have already been
64 already cultivated industrially (lipid-rich, robust etc.). This data alone cannot support a
65 comprehensive assessment of the future consequences of the microalgae sector's development
66 which could potentially take as many paths as there are microalgal strains and promising
67 compounds to be discovered via bioprospecting. Furthermore, while previous bioengineering
68 studies[28,29] model the potential for microalgal productivities in different PBRs and locations,
69 previous LCA studies only assess productions localized in one or a few sites. Yet, it is reasonable
70 to assume that an increase in demand for new microalgal compounds would, in the long run, result
71 in the supply of microalgae from several different locations with distinct productivities,
72 thermoregulation needs, and electricity mixes. In fact, 447 microalgae or cyanobacteria farms are
73 already active in 23 European countries[30].

74 Forecasting the environmental consequences of future developments in the European microalgae
75 sector therefore requires extending the scope of the previous assessments to include many possible
76 scenarios. This immense number of possibilities is inherent to bioprospecting, which implies that
77 the desired property of a bioprospected compound is known (for instance an anti-inflammatory
78 compound), but not the organism which will produce it. Besides the case of bioprospecting, it is
79 common[31] to consider a large number of scenarios in ex-ante LCA as it aims at anticipating the
80 environmental impact of emerging technologies before these are actually implemented at industrial
81 scale[32]. A major challenge in ex-ante LCA is thus the need to generate Life Cycle Inventories
82 (LCI) for future production systems which currently exist only at a low level of technological and
83 market maturity[33] such as pilot scale applications. In a recent review of common practices in ex-
84 ante LCA[31], one third of the 18 included studies resorted to process simulation to obtain LCIs at
85 an industrial scale, mainly using technology-specific simulation software. In the case of microalgal

compounds which are still being bioprospected, the upscaling anticipation can be done using parameterized physical and biological models to simulate photobioreactors and strains in different conditions. In fact, it is common practice[18,21,23–25,27,34] to simulate inventories for LCAs in the microalgal sector and recent studies show advanced models taking various biophysical phenomena into account[35]. Microalgae LCA models with extensive parameterization can be found associated with some forms of uncertainty and sensitivity analysis via stochastic sampling[14,34,36].

These parametrized models, however, cannot cover the scope of possibilities associated with a microalgal compound that is not found yet, and whose production upscaling and development in a European production market are indeterminate. Yet, the consequences of an increase in demand for high value microalgal compounds must be assessed early on to inform both policy makers in the sustainability domain and the microalgal sector. The ex-ante assessment should put these stakeholders in a better position to evaluate the likelihood of microalgal high-value compounds' environmental superiority over alternatives as well as to identify the optimal scenarios and try to aim for them.

To do so, the present work aims at investigating the impacts of an increase in demand for a microalgal compound with a desired property that is currently being bioprospected in Europe (a bioprospected microalgal compound). The uncertainty space associated with this technological development is shaped by several forms of uncertainty that can either be epistemic i.e. due to a lack of knowledge, or aleatory because stemming from inherently random processes[37]. We build on previous work[38] developing a parameterized model to simulate the microalgae cultivation technology from a life cycle perspective. The "techno operational uncertainty" addressed in this previous work is due to the impossibility of accurately predicting the productivity of a new specific strain in a specific photobioreactor and location. To tackle our research question, we here need to

extend the parameterized model and the scope of previous LCAs in the microalgal sector to include other sources of uncertainty, namely the lack of knowledge about the exact nature of the strain and the bioprospected compound, the associated PBR, and the geographic developments of the market. We anticipate that despite these large uncertainties, the stochastic propagations will provide insightful density-based representations of the environmental consequences of an increase in demand for yet undiscovered microalgal compounds. This work also contributes to the developments and discussions around uncertainty, global sensitivity analysis and the associated terminologies in the field of ex-ante LCA.

2. Methods

The approach consists in applying stochastically generated samples to our previously developed parametrized LCA model[38] on which minor changes were made (cf. 2.1) to assess the impacts for an increase in demand and production of 1 kg of bioprospected compound in Europe. The whole model is coded on Python 3.8 with the LCA package Brightway2[39] and is available on GitHub[40]. The background database is the consequential version of Ecoinvent 3.6. The impact assessment categories are Global Warming with a 100-year time horizon (GW100), Freshwater Eutrophication (FE), Water Depletion (WD) and Terrestrial Ecotoxicity (TETinf) from ReCiPe Midpoint (H) V1.13.

2.1 Deterministic model and LCA framework

The functional unit is 1 kg of bioprospected compound. Consequential LCA modeling was chosen as, by looking at the future effects of decisions, and including only activities and technologies expected to be able to respond to future changes in demand, the consequential approach is prospective in nature and therefore well-suited to the assessment of emerging technologies.

Moreover, the consequential approach reduces the number of normative assumptions needed, and since it is highly speculative to anticipate normative preferences in the future, this can be argued to be an advantage when performing ex-ante LCA. The foreground product system includes the cultivation of microalgae in an outdoor vertical tubular PBR with the associated energy consumptions for water pumping, mixing, thermoregulation by a heat pump and centrifugation for biomass harvesting. The product system also comprises nutrients, CO_2, water, and glass consumptions. The extraction of the compound is not modeled but cell disruption is accounted for as it likely constitutes the first step of the post-harvest processing, regardless of the biochemical class of the compound (protein, lipid, carbohydrate)[41,42]. Drying is modeled for the whole biomass so that the co-produced biomass (dependent co-product) is ready to substitute functionally equivalent products already on the market. The cultivation technology and the foreground product system are described in detail in SI I.2 and in our previous work and model[38], for which a few modifications were made to the product system. First, thermoregulation of the PBR was assumed to be provided by a reversable heat pump[43] with a Coefficient of Performance (COP) of 3, which we chose as an average value over locations and seasons, instead of electric heating and a fluid thermal exchanger. Additionally, considering multiple potential strains with different characteristics made it necessary to model two additional possible substitution routes for the co-produced biomass (cf. SI I.3). This biomass can now enter the animal feed energy and feed protein markets[44], or be directly incorporated in fish feed after modification of the reference fish feed composition as previously modeled[38]. As a third possible substitution route, the co-produced biomass can be digested in an anaerobic digester for biogas production and substitution on the biogas marginal market based on a functional unit of 1MJ of heating capacity. The biogas yields depend on the composition of the microalgal strains (cf. SI I.3.2.2).

The life cycle inventory results from a simulation of microalgal cultivation assumed from April to September within Europe. This simulation and the LCI result from the interaction of 27 parameters characterizing the strain and its compound, 22 techno-operational parameters characterizing the cultivation technology, the PBR geometry and setup, 3 geographic parameters defining the location, and 6 physical parameters. The cultivation simulation uses climatic data from the Photovoltaic Geographic Information System (PVGIS)[45]. The simulation, its modules, the parameters, and all the equations are detailed in our previous work[38] and in SI I for the additions and modifications.

2.2 Types of uncertainty and assumptions

2.2.1 Bioprospecting uncertainty

The "bioprospecting uncertainty" is caused by the lack of knowledge about the strain and the compound that will be found to feature the desired property (for instance anti-inflammatory) and successfully upscaled after bioprospecting. The bioprospecting uncertainty is epistemic[37] in the first place as it stems from the lack of knowledge about which kinds of microalgal strains or compounds classes (lipid, carbohydrate, protein) are more likely to possess the desired property. , We have assumed that all strains and types of compounds have equal probabilities to possess the desired property, as we currently lack arguments and data to hypothesize potential correlations between biological traits and desired properties. Therefore, the bioprospecting process was modeled as a random draw within microalgal biodiversity, whose result is subject to aleatory uncertainty. This is conceptually analogous to a draw in an opaque urn in which the balls would be the strains and their compounds whose proportions in the box depend on our knowledge on biodiversity(cf. 3.3).

To do so, we first use 27 parameters defining a "strain-compound pair", i.e. a specific compound hosted in a specific strain. Some parameters define biological characteristics such as biomass composition, nitrogen source, or photosynthetic efficiency. Other parameters define if the strain-compound pair requires PBR thermoregulation at night or characterize the fate of the co-produced biomass (biogas, fish feed, or animal feed) that we consider strain-specific because depending on cell wall characteristics, digestibility, toxicity etc.[46–48] Finally, compound-specific parameters define respectively: whether the bioprospected compound is a lipid, protein, or carbohydrate, i.e. the biochemical class of the compound; and the mass fraction of compound in such class, for example measured as the mass of compound per total mass of proteins in the strain if the compound is a protein. The values of these compound-specific parameters are also characterized by uncertainty which means that the same functional unit of 1 kg of bioprospected compound can be provided by different reference flows of cultivated microalgal biomass.

We modeled the random draw within the microalgal biodiversity by sampling random values for the parameters for which variation ranges are reported in the literature for the microalgal biodiversity (23 out of 27 parameters, cf. SI II.1). For 17 parameters out of 23, we modeled a uniform distribution within the range in lack of further arguments to use other distributions.

2.2.2 Techno-operational uncertainty

This epistemic uncertainty was specifically addressed in our previous work[38] and is due to the unpredictable behavior and growth of a strain defined by its biological parameters in a specific vertical tubular PBR and location. More precisely, we used the model from Williams and Laurens (2010)[28] which estimates a maximum areal yield ($g_{dw} \cdot m^{-2} \cdot d^{-1}$) depending on the ground horizontal irradiance ($kJ \cdot m^{-2} \cdot d^{-1}$) and the strain-specific theoretical energetic yield ($g_{dw} \cdot kJ^{-1}$). Since

Williams and Laurens (2010)[28] observe that real cultivations in PBR would often reach 30% of this maximum yield, in this study the techno-operational uncertainty refers to the lack of knowledge about which PBR geometry and operational set-up will enable the modeled strain to reach this percentage. The techno-operational uncertainty was addressed by simulating random values of geometrical (e.g. tube diameter and distance between tubes) and operational (flow rate, biomass concentration) parameters defining the PBR for a strain and location. The values were sampled within ranges reported in the literature for different vertical tubular PBRs with different strains in various locations (cf. SI I.1). The sampled combinations were all assumed to have equal chances of enabling the strain to reach 30% of its maximum yield.

In addition to the geometrical and operational parameters, the uncertain vertical distance between the water source (river or well) and the PBR, and the wind-dependent convective exchange coefficient ruling the thermal exchange between the PBR and the surrounding air were included in the techno-operational uncertainty.

In total, 7 techno-operational parameters are therefore considered uncertain.

2.2.3 Geographic locations and uncertainty of production mix

Similarly to any agricultural crop for which an increase in demand in Europe will be answered by different producers in distinct locations (a mix), an increase in demand for the bioprospected compound will be met by distinct microalgae plants in Europe belonging to a "compound production mix". To anticipate the development of this compound production mix in Europe, we first assumed that the production would take place in the 10 countries which have the highest potential for microalgal biomass production as identified by Skarka[49]: Spain (ES), Sweden (SE), Italy (IT) , Portugal (PT), United Kingdom (UK), France (FR), Greece (EL), Cyprus (CY), Ireland

(IE) and Germany (DE). The author identified these countries as the best combinations of temperature, solar irradiance, and available land after exclusion of urban, mountainous, and protected areas. To account for indeterminacy regarding the plants' locations, a grid was first generated with random locations drawn every 2° of latitude in each country (28 locations in total). Mono-dimensional sampling was performed in each of this location, while multi-dimensional sampling only could add production mix uncertainty by sampling production mixes within the grid (cf. 2.3). To do so, random combinations of locations were selected within the grid in three different scenarios regarding the spread of the mix over Europe. Thus, in these scenarios, 5, 15, or 25 locations out of 28 were assumed to answer to the increase in demand.

In consequential LCA, the identification of the marginal suppliers and their shares in the mix are based on the study of market trends, that are shaped by both political and economic factors[50,51]. In our case, due to the lack of data on market performance we used areal productivity as a proxy and assumed that the plants in locations with higher areal productivities will have a higher chance to be part of the compound production mix. We then assumed equal production shares within this mix, once its locations have been determined: each plant produces 200 g of compound in a production mix for 1 kg if the mix contains 5 plants in different locations. A country-specific electricity mix was used when simulating each plant.

2.2.4 Independence assumptions

The model was designed so that the sampled parameters are independent. For instance, our knowledge does not indicate if a specific strain has a higher chance to grow on nitrate instead of ammonium if it has a high optimal temperature and a short cell diameter. These three parameters were therefore sampled independently. Similarly, a cell diameter does not indicate if the strain has

246 a higher chance to grow at the expected yield in a certain tube diameter, all other things being
247 considered. Indeed, we did not model direct dependence between techno-operational parameters
248 and productivity for a strain but instead treated this complexity as a part of the uncertainty (cf.
249 2.2.2) that could be reduced with more knowledge on the dependencies observed across species
250 and locations. On the contrary, resorting to a parameter defining the content of the bioprospected
251 compound in the biomass which would be independent of the biomass composition would lead to
252 unrealistic scenarios. Thus, the biomass composition was first generated by randomly sampling a
253 lipid content of the ash-free dry biomass and an ash content, from which the rest of the composition
254 is calculated[28], and the bioprospected compound constitutes a random fraction of a random
255 biochemical class (lipid, protein, carbohydrate).
256
257 ***2.3 Sampling strategies for uncertainty propagation and sensitivity analysis***
258 As illustrated in Figure 1, we implemented two random sampling strategies to propagate the
259 uncertainty and perform sensitivity analysis.
260 The first strategy named "mono-dimensional sampling" mixes all types of uncertainties
261 previously described (bioprospecting, techno-operational, cf. 2.2) by applying Sobol sampling to
262 all parameters. With this sampling strategy, we obtained for each location of the grid 114688
263 random combinations of the 23 biological and 7 uncertain techno-operational parameters. The
264 global sensitivity analysis associated with mono-dimensional sampling allows ranking all
265 parameters based on their influence on the dispersion of the impact scores in one location.
266 To be able to simulate the development of European production mixes producing the same
267 strain-compound pairs in different locations, the second sampling strategy, namely "multi-
268 dimensional sampling", differentiates between uncertainty types. We first generated a Sobol

sample to obtain a set of 5376 strain-compound pairs that could potentially display the desired property (bioprospecting uncertainty). The cultivation and production of each strain-compound pair was then simulated for each of the 28 locations of the grid, in 150 random PBR geometries and operational setups generated with Monte Carlo sampling on the 7 uncertain techno-operational parameters (techno-operational uncertainty). As the same strain-compound pairs were simulated in all locations of the grid, we could generate production mixes for all pairs by composing 400 random combinations of locations on the grid (Production mix uncertainty). The probabilities for each location to be part of the marginal mix were weighted with the areal productivities (cf. 2.2.3). Unlike mono-dimensional sampling, multi-dimensional sampling allows assessing the uncertainty associated with the environmental impact caused by an unknown European production mix producing the same strain-compound pair, after aggregating techno-operational uncertainty (cf. Figure 1). This sampling strategy also allows studying how sensitive is the impact of the entire European production mix (composed of the 28 locations of the grid) to the bioprospecting uncertainty, i.e. to the parameters defining the strain-compound pair produced in this mix.

The global sensitivity analyses were performed with the Sobol methods from the python Salib package[52].

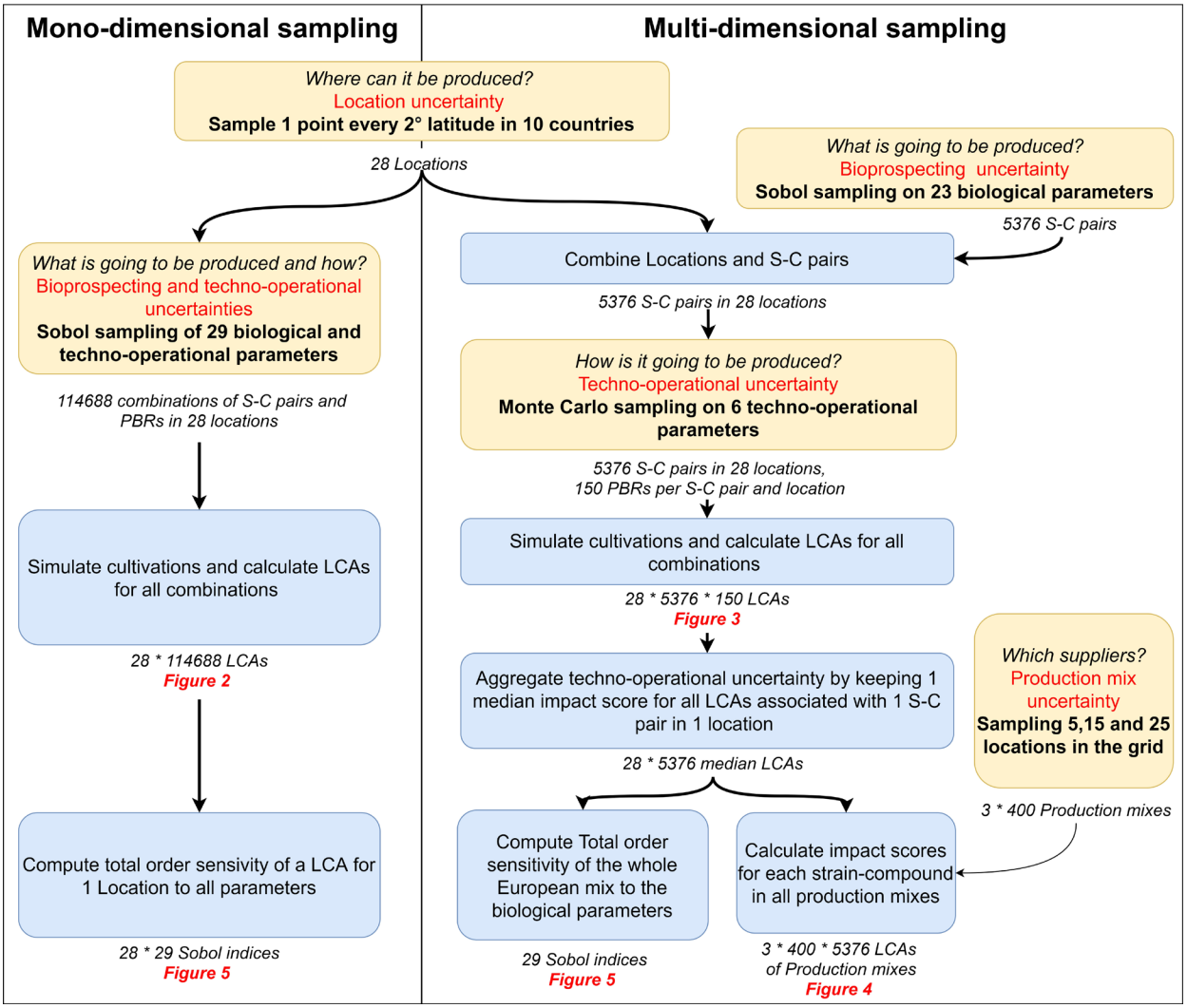

Figure 1: Visualization of the sampling strategies and the associated calculations. *Acronyms: S-C= Strain-Compound. Blue and orange boxes respectively indicate a calculation step and a sampling step. We indicated the figures of the article under the results that they display.*

3. Results and discussion

3.1 Uncertainty propagation with mono-dimensional sampling

The first notable observation is that the propagation of the uncertainty resulted in a very wide range of impacts scores, with for instance the global warming impact (GW100) per kg of bioprospected compound ranges from -100 to +89000 kg CO_2-eq / kg compound with mono-dimensional sampling (cf. SI I.3). This very large dispersion is mainly due to the uncertain content of bioprospected compound in the biomass, which is part of the bioprospecting uncertainty. The bioprospected compound content is a secondary parameter as it results from the interaction of four uncertain primary parameters (cf. 2.2.4). The propagation of the uncertainty for these four parameters resulted in a target compound content ranging from 0.001 to 0.6 $g \cdot g_{driedbiomass}^{-1}$ (cf. SI II.2). The highest impact score in the range corresponds to extremely unfavorable conditions: a very low content of bioprospected compound in the biomass (0.002 $g \cdot g_{driedbiomass}^{-1}$), coupled with a northern location (Sweden), a high strain-specific thermal range and a large PBR volume involving low volumetric productivity and substantial PBR heating requirements. GW, Freshwater Eutrophication (FE), and Water Depletion (WD) impact scores all increase when the target compound content decreases because of a need to produce more biomass to provide the same functional unit, but a lower target compound content induces a higher Terrestrial Ecotoxicity (TET) impact on average (Figure 2). The observed overall trend in Figure 2 however hides the specific trends for the three equiprobable substitution routes. Indeed, the overall trend is only due to the scenario in which the coproduced biomass substitutes fish feed. Despite constituting one third of all the simulations, the strong positive slope observed for this scenario outweighs the slightly negative slope for the two other scenarios, which results in the trend observed in Figure 2

317 (cf. Figure S13 in SI I. 4.2.4.1). Fish feed substitution almost always implies negative TET scores
318 (positive impact on the environment), which is partly the case for animal feed and never happened
319 for biogas substitution. The environmental superiority of fish feed substitution over biogas
320 production had also been found in a previous study[24].

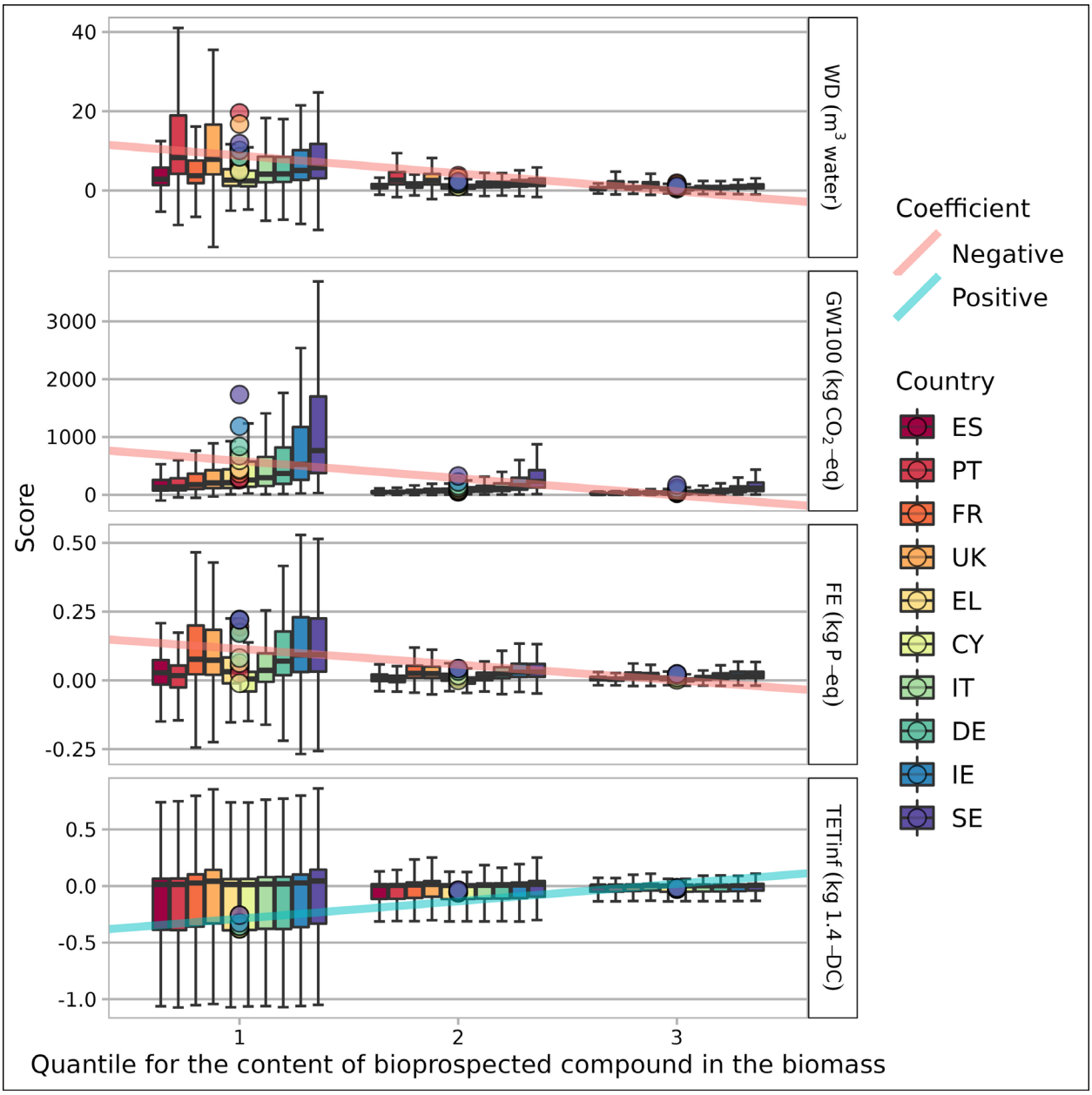

Figure 2: Boxplot of the environmental scores obtained in mono-dimensional sampling. *The 3 211 264 LCA scores resulting from mono-dimensional sampling are divided into 3 quantiles applying to the dispersion of the uncertain bioprospected compound content in the biomass. Boundaries of the quantiles ($g_{bioprospected\ compound} \cdot g_{driedbiomass}^{-1}$): 0-001-0.090,0.090-0.185,0.185-0.60. The dots indicate the average scores per country. The regression lines are only displayed to highlight the bioprospected compound content influence on the scores. The equations of the lines*

328 *are Score=coeff*Q+intercept, with Q the quantile numbers 1,2, and 3. More detailed plots can*
329 *be found in SI I.4.2.4.1. WD= Water Depletion, GW100=Global Warming with a 100-year time*
330 *horizon, FE=Freshwater Eutrophication, TETinf=Terrestrial Ecotoxicity.*

331

332

333

334

335

336

337

338

339

340

341

342

3.2 Uncertainty propagation with multi-dimensional sampling

3.2.1 Bioprospecting and Techno-operational uncertainties

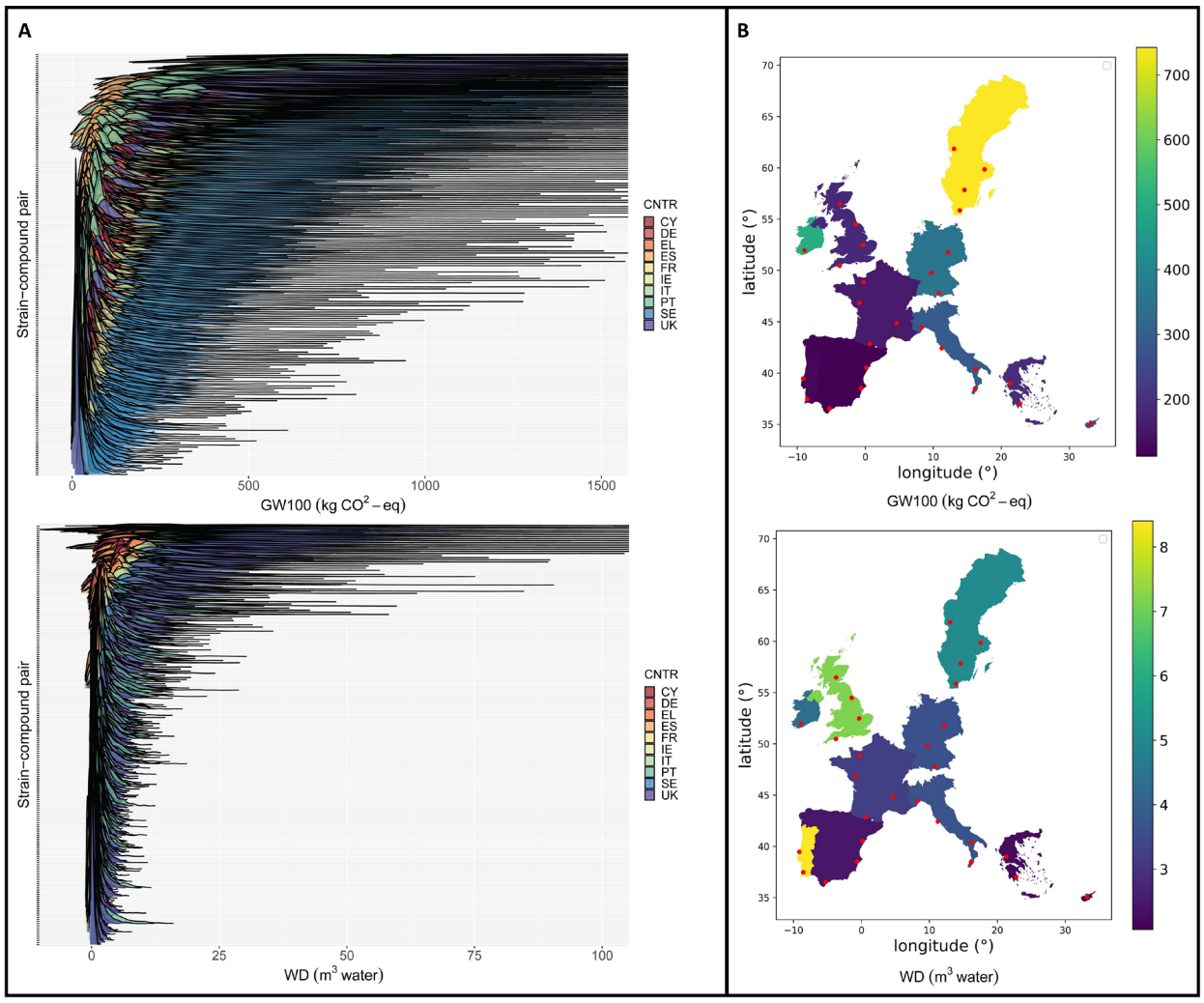

Figure 3: (A)Distinction of uncertainties with strain-compound-specific ridgelines and (B) Mapping of average impacts scores per country. (A) *Each horizontal line corresponds to one strain-compound pair for which the LCA scores in different locations and stochastically generated PBRs constitute the density curves. The plots only show 200 of the 5376 randomly generated strain-compound pairs in multi-dimensional sampling. The strain-compound pairs were divided into 200 quantiles regarding the dispersion of the GW impact scores and one pair was chosen per quantile and displayed on the figures.* ***(B)*** *The color gradients indicate the mean impact score per*

country, considering all simulations performed in each country. The red dots indicate the 28 locations of the randomly generated grid. The figures for TET and FEP are shown in SI I.4.1.

In Figure 3, for each horizontal line representing a strain-compound pair, the density curves of the impact (horizontal axis in Figure 3) result from the propagation of the techno-operational uncertainty in the different countries. Despite a visible shift of the impact density curves across strain-compound pairs (vertical axis in Figure 3) and different countries (different colors in Figure 3), the significant overlap between strain-compound pairs indicates a large influence of techno-operational uncertainty.

It must be noted for GW, FE, and WD, that the shifts of the curves along the horizontal axis are not mere linear transposition of the density curves but are associated with a higher standard deviation of the results for strain-compound pairs with higher average impact scores (cf. SI I.4.3). In other words, the dispersion of the impact scores due to techno-operational uncertainty varies with the modeled strain-compound pair. This heteroskedastic statistical behavior stems from two mechanisms particularly visible for GW. First, the same techno-operational input uncertainty is assumed for the cultivation simulations of all strain-compound pairs, which tends to result in a constant coefficient of variation (*Standard deviation/Mean*) and therefore a linear increase of the standard deviation across the mean impact scores of different strain-compound pairs (cf. Figure S16, SI I.4.3). Second, the coefficient of variation is tendentially higher for strains with higher optimum temperatures of culture (cf. Figure S15, S16, S20, SI I.4.3), which are also associated with high impact scores on average. This phenomenon was observed in our previous work[38] and stems from the fact that techno-operational uncertainty propagates more when thermoregulation can become a hotspot due to the combination of strain's thermal requirements and location.

375

376 *3.2.2 Variability across countries and production mix uncertainty*

377 Despite techno-operational and bioprospecting uncertainties which cause substantial overlap
378 between impact density curves (Figure 3.a.), the ten countries can be ranked according to the
379 average impact score for all simulations (Figure 3.b. and also observed in Figure 2 with mono-
380 dimensional sampling). Latitude is an important determinant of the environmental impacts (cf.
381 Figure S5, SI I.4.2.1.1) as it affects the horizontal irradiance and therefore influences biomass
382 productivity. Latitude also determinates the outside temperature and therefore the energy required
383 to thermoregulate the culture, in particular heating requirements, which was highlighted as an
384 environmental hotspot in other studies[38,53,54]. Thus, the impact scores for all impact categories and
385 countries tendentially increase with the strain-specific optimal temperatures *Topt* (part of the
386 bioprospecting uncertainty), and the regression slopes associated with *log(Impact score) = f(Topt)*
387 are higher for northern countries (cf. SI I.4.2.1.2). Additionally, the impact scores per FU are
388 strongly influenced by the impact profiles of the national electricity mixes (cf. SI I.4.2.2). To make
389 an example, despite of its southern location, production in Portugal is associated with the highest
390 WD impact score among all countries due to the high WD impact of the Portuguese electricity mix
391 (Figure 2,3). However, it is important to note that current marginal mixes used in consequential
392 modeling only have a limited period of validity in the near/medium term future.

393 Differences between the impact scores of distinct countries do not necessarily imply additional
394 uncertainty for the impact scores associated with the production of 1 kg of bioprospected
395 compound produced by a European production mix. Figure 4 shows how the dispersion of the
396 impact scores for the strain-compound pairs varies across the generated production mixes. The
397 differences observed between the distributions, which illustrate the production mix uncertainty,

398 shrink when more locations are considered per mix. Indeed, the more locations there are in the
399 randomly generated mixes, the closer the latter get to a full European mix composed of the 28
400 locations of the grid.

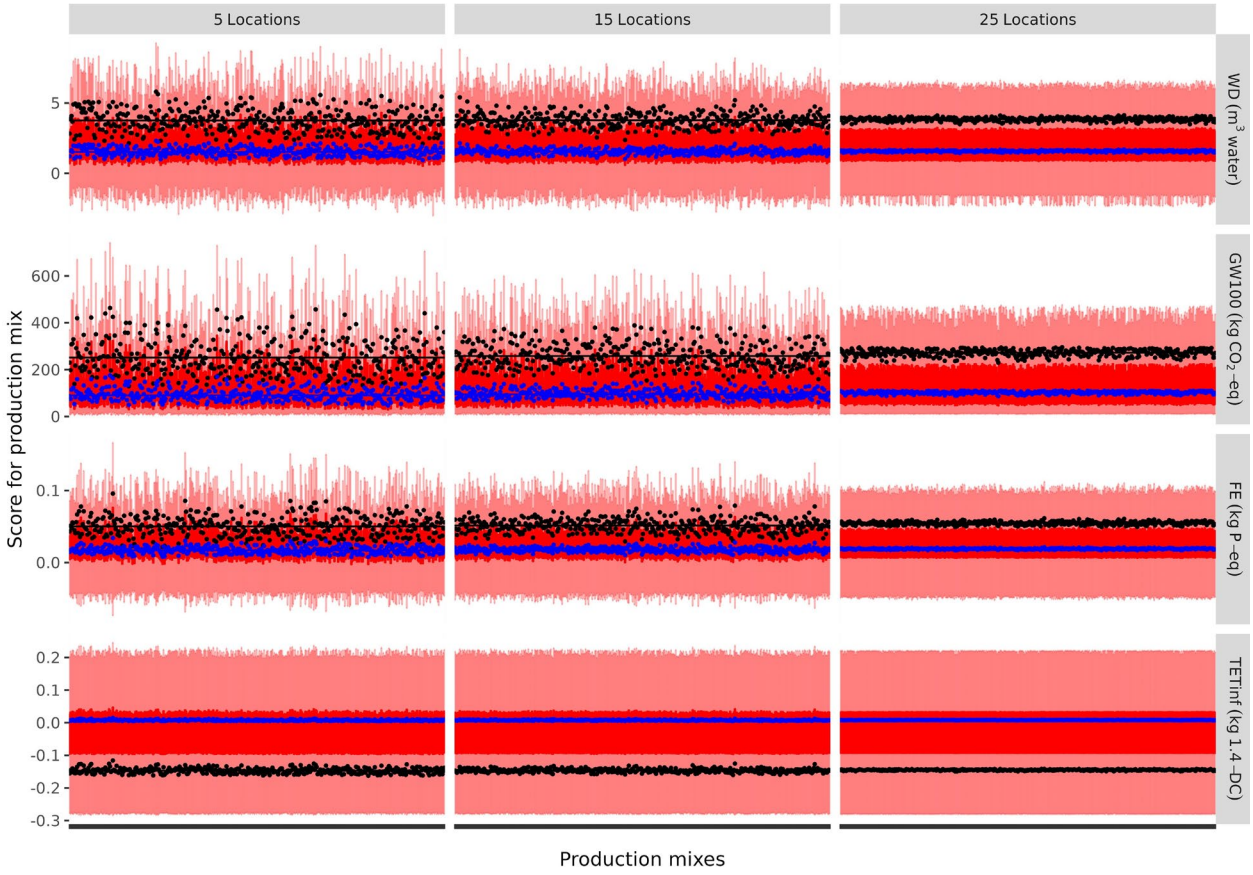

401

402 ***Figure 4: Production mix and bioprospecting uncertainties in aligned boxplots.*** *The red area*
403 *consists of a succession of narrow boxplots along the horizontal axis corresponding to 400*
404 *randomly generated production mixes. The range of each boxplot on the vertical axis corresponds*
405 *to the dispersion of impact score per strain-compound pair produced in the production mix. The*
406 *impact score for a strain-compound i in the production mix p is calculated as follows:* $SMimp_{p,i} =$
407 $\frac{\sum_{L=0}^{N_p} Median(\left[imp_{i,L,0}\ ,\ldots,\ imp_{i,L,a}\ , imp_{i,L,150}\ \right])}{N_p}$, *with Np the number of locations in the production mix p, L*
408 *the identifier of a location being part of p and* $imp_{i,L,a}$ *the impact score calculated for the*

production of strain-compound pair i, in location L and in PBR a. The black and blue dots respectively indicate the means and medians of each boxplot. The horizontal black and blues lines respectively represent the mean across boxplots and the means of the medians across boxplots.

3.3 Sensitivity Analysis

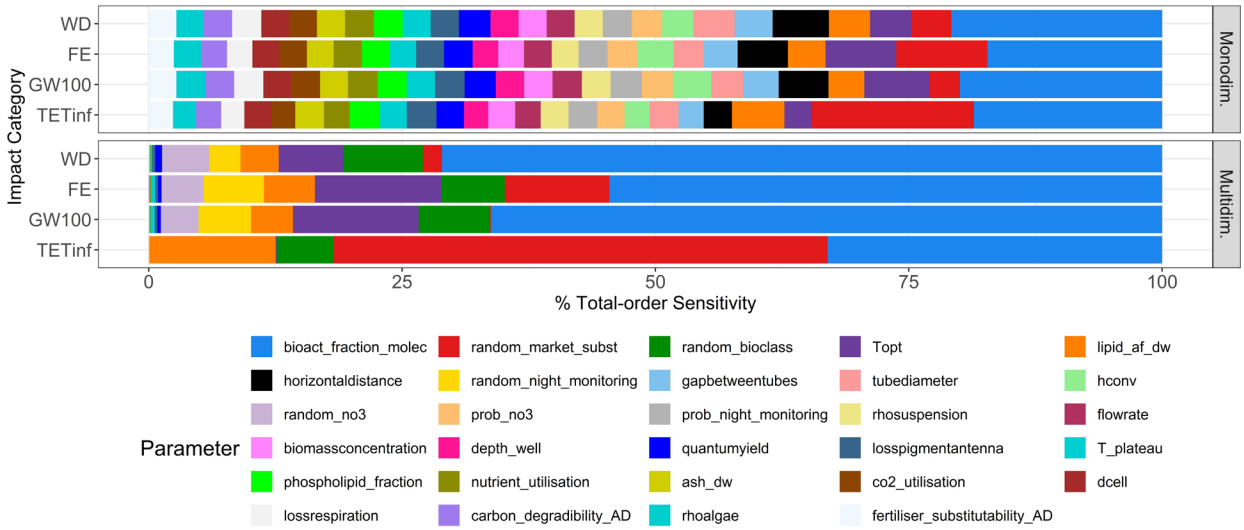

Figure 5: Shares of the Sobol total-order sensitivity for the uncertain parameters in multi-dimensional and mono-dimensional samplings. *The parameters are detailed in SI II.1. In mono-dimensional sampling the share of the total-order sensitivity for a parameter x is calculated as* $Share_x = \frac{\frac{\sum_{L=0}^{28} Indice_{x,L}}{28}}{\sum_{i=0}^{p}(\frac{\sum_{L=0}^{28} Indice_{i,L}}{28})}$*, with* $Indice_{x,L}$ *the total-order sensitivity indice calculated in location L for parameter x, and p the number of uncertain parameters in mono-dimensional sampling. In multi-dimensional sampling,* $Share_x = \frac{Index2_x}{\sum_{i=0}^{p} Index2_i}$ *with* $Indice2_x$ *the total-order sensitivity index*

420 *of the biological parameter x associated with the impact for a strain-compound in Europe (cf.*
421 *Figure 1). The error bars and dispersion of the different indexes are shown in SI I.5.3.*

422 Mono-dimensional and multi-dimensional samplings allow for a multifaceted understanding of the
423 model's sensitivity to the different parameters. Regarding the impact scores associated with one
424 strain-compound pair in one location, Figure 5 shows for mono-dimensional sampling that the
425 uncertainty on the fraction of bioprospected compound in the biochemical class (lipid,
426 carbohydrate, protein) dominates in the output uncertainty for all impact categories. This was
427 expected as this parameter eventually affects the overall content of bioprospected compound in the
428 biomass and therefore substantially influences the reference flows in the product system. The
429 uncertainty on the parameter assigning the substitution route also dominates the output uncertainty
430 for TET and FE, which is to be put in relation to the significantly different LCA profiles of the
431 three substitution routes (cf. 3.1 and Figure S13 in SI I.4.2.4.1, SI I.4.2.3). Eventually, the techno-
432 operational uncertainty on the geometry of the PBR and the resulting culture volume (tube
433 diameter, horizontal distance between stacks, gap between tubes) accounts for 15-20% of the
434 output variance for all impact categories. As also described in our previous work[38] this is mainly
435 due to the influence of the PBR volume on the thermoregulation requirements, together with the
436 strain's thermal requirements (*Topt*, *Tplateau*) and location. The 22 other parameters explain
437 around 60% of the output uncertainty, which makes it difficult to decide on which parameters
438 could be fixed to a unique value without losing information on the output uncertainty.

439 While mono-dimensional-sampling can spot uncertainty hotpots in the details of the model at the
440 techno-operational level, only multi-dimensional-sampling can investigate the sensitivity of the
441 model to a strain-compound pair at the European production level.

The latter as well shows that the fraction of bioprospected compound in the biochemical class (*bioact_fraction_molec*) and the parameter assigning the substitution route (*random_market_subst*) dominate the output uncertainty (75 %). The similar ranking of the common parameters between mono and multi-dimensional sampling shows that the same strain-compound-specific parameters strongly influence the impact scores for a production both in a unique location and when the same strain-compound pair is produced all over Europe.

Interestingly and in accordance with former observations (cf. 3.1), almost 100% of the output uncertainty for TETinf comes from the substitution mechanisms, determined by the biomass composition and substitution route. Thus, one could theoretically provide an educated estimate of the future TETinf impact of the production in Europe as soon as the biomass composition and the substitution market for a newly found strain-compound are known. Nevertheless, this estimate should be done keeping in mind the sensitivity of the model at the techno-operational level revealed by the mono-dimensional sampling.

3.3 Reflecting on Variability and Uncertainty

In this work, we have consistently used the word "uncertainty" to qualify the need to resort to a stochastically sampled set of values instead of using a static set of values for the parameters of our LCA model. The distinction between variability and uncertainty is key within the LCA community and more generally in modeling disciplines which cannot settle for a mere deterministic assessment to support decision-making[55–57]. While variability is intrinsic to real-world phenomena and processes, uncertainty is often defined as being due to a lack of knowledge about the model and its parameters[56–58]. This semantic overlapping between variability and uncertainty depending on the formulation of the research question is well described by Frey[55]. Our case confirms and illustrates how uncertainty and variability merge in some cases, depending on the research

question. The geographic variability becomes production mix uncertainty in our ex-ante LCA, as it stems from an irreducible lack of knowledge a priori about the future development of the mix. Similarly, while there is a vast diversity of microalgal strains and compounds, this biological variability translates into uncertainty associated with our research question about the impacts of an increase in demand for ***a*** microalgal compound that is currently being bioprospected in Europe. The uncertainty is here similar to the one applying to the result of a random draw (aleatory uncertainty) within a diverse population expressing variability (the biodiversity). Finally, the techno-operational conditions should also be understood as part of the uncertainty rather than just variability, as generating random PBR geometries and setups does not aim at representing alternative routes for a same compound production[57], but instead represent equiprobable scenarios for one strain to reach a specific productivity according to our limited knowledge.

To go further, the multi-dimensional strategy uses two independent loops as in the two-dimensional Monte Carlo simulation proposed by Michiels and Geeraerd[56] to distinguish variability and uncertainty. The difference is that we use this approach to distinguish bioprospecting uncertainty from techno-operational and production mix uncertainty. By doing so, we neglect biological variability by assuming that, once found and cultivated in a European mix, a strain does not express any phenotypical or genomic plasticity and features the same biological parameters' values in all locations. This is an oversimplification as the same strain producing the same compound in a European mix could for instance accumulate more or less lipids for different locations due to different light regimes[59]. In this sense, mono-dimensional sampling, while making impossible to distinguish between the types of uncertainty, also tackles a less fixist[60] and therefore more realistic concept of "microalgal strain" by simulating a continuum of biological parameters in a continuum of different PBRs and locations.

3.4 Limits

Our forecast partly relies on our choices regarding the modeling of microalgal biodiversity. Adapting the generic model from Williams and Laurens[28] to represent a strain could be argued to be simplistic and not cover the immense diversity of microalgae. For instance, sinking rates can in reality vary from the Stokes' law estimates we used to estimate centrifugation energy consumption[61], depending on the microalgal taxa and cell shapes[62]. Adapting the centrifugation technology may be necessary for some strains[63]. Furthermore, using ranges and distributions for the biological parameters based on results obtained within the known biodiversity to simulate undiscovered strains could be a good example of survivor bias[64]. In fact, we believe this bias benefits the representation of uncertainty by taking into account the demonstrated difficulty to cultivate many strains which can be observed in their environment[65,66]. The discovered and upscaled strain will therefore likely be relatively similar to the ones we already know. Finally, and as previously mentioned (cf. 2.2.2), the model would benefit from further refinement of the interactions between techno-operational, biological and geographic variables to limit the weight of unlikely combinations in the uncertainty representation.

3.5 Use of the results for decision-making

The high dispersion of the results associated with a very *large LCA space*[67] and the complex overlapping of the uncertainties must lead us to question the usability of the estimates for decision making. Ideally, the results should be used for planning and providing insightful indications on whether this technology will likely be beneficial and compete with alternatives. We can summarize the results by using the median impact score per kg of bioprospected compound across production mixes and strain-compound pairs: 1.5 m^3 for WD; 96 kg CO_2-eq for GW; 0.017 kg P-eq for FE and 0.007 kg 1.4-DC-eq for TET (cf. Figure 4 and Table S3 in SI I.3 for complete statistical

511 description). These values, however, are obtained by keeping one median score per strain-
512 compound pair and location, thus aggregating techno-operational uncertainty (cf. Figure 1). A first
513 comparison of magnitudes can be made with other bioactive compounds such as drugs from
514 industrial chemistry whose impacts can range from 30 to 3000 kg CO_2-eq per kg of drug[68]. Overall,
515 if a solution based on a bioprospected microalgal compound was to be compared with an
516 alternative technology for decision-making prior to technology development, the whole
517 distribution of the results should be considered and different statistical measures could be used[69]
518 (cf. SI I.3).

519 It must be highlighted that the results presented in this article can be understood as a *null model*
520 by analogy with its use in ecology[70]. Thus, the patterns of the model's output densities are obtained
521 for a set of standards assumptions associated with our current level of knowledge. Additionally,
522 the understanding of the uncertainty propagation combined with the sensitivity analysis allow
523 anticipating the shape of the densities when other assumptions are made or more knowledge is
524 gained. A key assumption supporting the *null model* is that bioengineers will find the combination
525 of photobioreactor geometry and operational setup associated with 30% of the strain-specific
526 energetic yields (cf. 2.2.1), as observed for cultivated strains by Williams and Laurens[28]. Running
527 the model with more pessimistic or optimistic assumptions regarding the capacity of bioengineers
528 to optimize photobioreactors for specific strains would shift the impact density curves. Another
529 assumption is that there is no restriction on the possible biochemical class of the target compound
530 (protein, lipid, carbohydrate) and content in the biomass. Finally, we do not account for market
531 mechanisms that could trim the density curves by making the worst cases economically non-viable,
532 for instance due to very high energy consumption per functional unit. This assumption can be

qualified as realistic as the context of high-value compounds does not exclude cases with high production costs provided that the market prices of the compounds follow.

4 Outlook

Through a heavy stochastic simulation of microalgae cultivations across strains, technological settings, and locations, this work demonstrates the use of computational resources to investigate the uncertainty associated with the future environmental impacts of a technology at very early stage. The stochastic approach, coupled with an explicit classification and separation of the uncertainties, allowed isolating the most important uncertain parameters but also to understand how techno-operational, bioprospecting and production mix uncertainties interact with each other. It is key to note that, by propagating uncertainty regarding the LCA of one bioprospected microalgal compound, our approach eventually drew the LCA profile of a whole biological group (microalgae) and its sector (productions of high-value microalgal compounds), in a whole market (Europe). An even more accurate LCA portrait of the microalgal high-value compounds sector would benefit from including background uncertainty, but also the extraction procedures which highly depend on the compound and strain. Overall, the approach can be generalized to technologies at a conceptual level of development for which the modelers know enough about the ruling biological and physical phenomena to determine the key model variables, draw dependencies, and eventually parameterize a model in which uncertainties are singled out. The value of the approach is enhanced when simultaneously applied to competing alternatives so that probability estimates resulting from the same method and same understanding of the uncertainties can be compared.

Finally, an additional step towards educated decision-making process and planning would be to use the model to go beyond the presented *null scenario* and propagate uncertainties using

556 prospective databases for market information and future marginal suppliers, but also climate
557 projections that could substantially influence the forecasts.

558

559

560 **ASSOCIATED CONTENT**

561 **"Supporting Information I"** (docx): Product system, description of additional calculations to the
562 model, additional figures, elementary composition of microalgal molecules' biochemical classes.

563 **" Supporting Information II"** (xlsx):

564 - **Sheet "SI II.1":** Table of parameters.
565 - **Sheet "SI II.2":** Statistical description of all model's outputs in mono-dimensional
566 sampling.
567 - **Sheet "SI II.3":** Correspondence between foreground activities and background
568 activities.
569
570

571 The code of the model allowing reproduction of the figures is available at
572 https://github.com/PJGilmw/Bioprospected_LCA[40].

573

574

575

576 **AUTHOR INFORMATION**

577 **Corresponding Author**

578 *Massimo Pizzol

Department of Planning, Aalborg University, Rendsburggade 14, 9000 Aalborg, Denmark

massimo@plan.aau.dk

FUNDING SOURCES

This research was carried out within the AquaHealth project, funded by the ERA-NET Cofund BlueBio program, grant no. 9082-00010.

ACKNOWLEDGMENT

The authors thank all members of the AquaHealth project for the insightful discussions around this work.

5 References

(1) Prokop, A.; Bajpai, R. K.; Zappi, M. E. *Algal Biorefineries: Volume 2: Products and Refinery Design*; 2015. https://doi.org/10.1007/978-3-319-20200-6.

(2) European Union. *BLUE BIOECONOMY LAST UPDATE: 2018 WWW.EUMOFA.EU Situation Report and Perspectives*; 2018. https://doi.org/10.2771/053734.

(3) García, J. L.; de Vicente, M.; Galán, B. Microalgae, Old Sustainable Food and Fashion Nutraceuticals. *Microb. Biotechnol.* **2017**, *10* (5), 1017–1024. https://doi.org/https://doi.org/10.1111/1751-7915.12800.

(4) Falaise, C.; François, C.; Travers, M.-A.; Morga, B.; Haure, J.; Tremblay, R.; Turcotte, F.; Pasetto, P.; Gastineau, R.; Hardivillier, Y.; Leignel, V.; Mouget, J.-L. Antimicrobial Compounds from Eukaryotic Microalgae against Human Pathogens and Diseases in Aquaculture. *Marine Drugs* . 2016. https://doi.org/10.3390/md14090159.

(5) Talero, E.; García-Mauriño, S.; Ávila-Román, J.; Rodríguez-Luna, A.; Alcaide, A.; Motilva, V. Bioactive Compounds Isolated from Microalgae in Chronic Inflammation and Cancer. *Marine Drugs* . 2015. https://doi.org/10.3390/md13106152.

(6) Yaakob, Z.; Ali, E.; Zainal, A.; Mohamad, M.; Takriff, M. S. An Overview: Biomolecules from Microalgae for Animal Feed and Aquaculture. *J. Biol. Res.* **2014**, *21* (1), 1–10. https://doi.org/10.1186/2241-5793-21-6.

(7) Talyshinsky, M. M.; Souprun, Y. Y.; Huleihel, M. M. Anti-Viral Activity of Red Microalgal Polysaccharides against Retroviruses. *Cancer Cell Int.* **2002**, *2* (1), 8. https://doi.org/10.1186/1475-2867-2-8.

(8) Huleihel, M.; Ishanu, V.; Tal, J.; Arad, S. (Malis). Antiviral Effect of Red Microalgal Polysaccharides on Herpes Simplex and Varicella Zoster Viruses. *J. Appl. Phycol.* **2001**, *13* (2), 127–134. https://doi.org/10.1023/A:1011178225912.

(9) Costa, J. A. V.; Freitas, B. C. B.; Cruz, C. G.; Silveira, J.; Morais, M. G. Potential of Microalgae as Biopesticides to Contribute to Sustainable Agriculture and Environmental Development. *J. Environ. Sci. Heal. Part B* **2019**, *54* (5), 366–375. https://doi.org/10.1080/03601234.2019.1571366.

(10) Kottuparambil, S.; Thankamony, R. L.; Agusti, S. Euglena as a Potential Natural Source of

620 Value-Added Metabolites. A Review. *Algal Res.* **2019**, *37* (November 2018), 154–159.
621 https://doi.org/10.1016/j.algal.2018.11.024.

622 (11) Arvidsson, R.; Tillman, A. M.; Sandén, B. A.; Janssen, M.; Nordelöf, A.; Kushnir, D.;
623 Molander, S. Environmental Assessment of Emerging Technologies: Recommendations for
624 Prospective LCA. *J. Ind. Ecol.* **2018**, *22* (6), 1286–1294. https://doi.org/10.1111/jiec.12690.

625 (12) Hans-O. Pörtner (Germany), Debra C. Roberts (South Africa), Helen Adams (United
626 Kingdom), Carolina Adler (Switzerland/Chile/Australia), Paulina Aldunce (Chile), Elham
627 Ali (Egypt), Rawshan Ara Begum (Malaysia/Australia/Bangladesh), Richard Betts (United
628 Ki, Z. Z. I. (Malaysia). *Climate Change 2022 - Impacts, Adaptation and Vulnerability -*
629 *Summary for Policymakers*; 2022.

630 (13) Lardon, L.; Hélias, A.; Sialve, B.; Steyer, J. P.; Bernard, O. Life-Cycle Assessment of
631 Biodiesel Production from Microalgae. *Environ. Sci. Technol.* **2009**, *43* (17), 6475–6481.
632 https://doi.org/10.1021/es900705j.

633 (14) Brentner, L. B.; Eckelman, M. J.; Zimmerman, J. B. Combinatorial Life Cycle Assessment
634 to Inform Process Design of Industrial Production of Algal Biodiesel. *Environ. Sci. Technol.*
635 **2011**, *45* (16), 7060–7067. https://doi.org/10.1021/es2006995.

636 (15) Clarens, A. F.; Nassau, H.; Resurreccion, E. P.; White, M. A.; Colosi, L. M. Environmental
637 Impacts of Algae-Derived Biodiesel and Bioelectricity for Transportation. *Environ. Sci.*
638 *Technol.* **2011**, *45* (17), 7554–7560. https://doi.org/10.1021/es200760n.

639 (16) Sills, D. L.; Paramita, V.; Franke, M. J.; Johnson, M. C.; Akabas, T. M.; Greene, C. H.;
640 Tester, J. W. Quantitative Uncertainty Analysis of Life Cycle Assessment for Algal Biofuel

641 Production. *Environ. Sci. Technol.* **2013**, *47* (2), 687–694.
642 https://doi.org/10.1021/es3029236.

643 (17) Connelly, E. B.; Colosi, L. M.; Clarens, A. F.; Lambert, J. H. Life Cycle Assessment of
644 Biofuels from Algae Hydrothermal Liquefaction: The Upstream and Downstream Factors
645 Affecting Regulatory Compliance. *Energy and Fuels* **2015**, *29* (3), 1653–1661.
646 https://doi.org/10.1021/ef502100f.

647 (18) Vasudevan, V.; Stratton, R. W.; Pearlson, M. N.; Jersey, G. R.; Beyene, A. G.; Weissman,
648 J. C.; Rubino, M.; Hileman, J. I. Environmental Performance of Algal Biofuel Technology
649 Options. *Environ. Sci. Technol.* **2012**, *46* (4), 2451–2459.
650 https://doi.org/10.1021/es2026399.

651 (19) Duran Quintero, C.; Ventura, A.; Lépine, O.; Pruvost, J. Eco-Design of Spirulina Solar
652 Cultivation: Key Aspects to Reduce Environmental Impacts Using Life Cycle Assessment.
653 *J. Clean. Prod.* **2021**, *299*. https://doi.org/10.1016/j.jclepro.2021.126741.

654 (20) Smetana, S.; Sandmann, M.; Rohn, S.; Pleissner, D.; Heinz, V. Bioresource Technology
655 Autotrophic and Heterotrophic Microalgae and Cyanobacteria Cultivation for Food and
656 Feed : Life Cycle Assessment. *Bioresour. Technol.* **2017**, *245* (August), 162–170.
657 https://doi.org/10.1016/j.biortech.2017.08.113.

658 (21) Schade, S.; Meier, T. Distinct Microalgae Species for Food—Part 1: A Methodological
659 (Top-down) Approach for the Life Cycle Assessment of Microalgae Cultivation in Tubular
660 Photobioreactors. *J. Appl. Phycol.* **2020**, *32* (5), 2977–2995.
661 https://doi.org/10.1007/s10811-020-02177-2.

(22) Porcelli, R.; Dotto, F.; Pezzolesi, L.; Marazza, D.; Greggio, N.; Righi, S. Science of the Total Environment Comparative Life Cycle Assessment of Microalgae Cultivation for Non-Energy Purposes Using Different Carbon Dioxide Sources. *Sci. Total Environ.* **2020**, *721*, 137714. https://doi.org/10.1016/j.scitotenv.2020.137714.

(23) Stephenson, A. L.; Kazamia, E.; Dennis, J. S.; Howe, C. J.; Scott, S. A.; Smith, A. G. Life-Cycle Assessment of Potential Algal Biodiesel Production in the United Kingdom: A Comparison of Raceways and Air-Lift Tubular Bioreactors. *Energy and Fuels* **2010**, *24* (7), 4062–4077. https://doi.org/10.1021/ef1003123.

(24) Posada, J. A.; Brentner, L. B.; Ramirez, A.; Patel, M. K. Conceptual Design of Sustainable Integrated Microalgae Biorefineries: Parametric Analysis of Energy Use, Greenhouse Gas Emissions and Techno-Economics. *Algal Res.* **2016**, *17*, 113–131. https://doi.org/10.1016/j.algal.2016.04.022.

(25) Powers, S. E.; Baliga, R. Sustainable Algae Biodiesel Production in Cold Climates. *Int. J. Chem. Eng.* **2010**, *2010*. https://doi.org/10.1155/2010/102179.

(26) Kadam, K. L. Microalgae Production from Power Plant Flue Gas: Environmental Implications on a Life Cycle Basis. *Contract* **2001**, No. June, 1–63.

(27) Axelsson, L.; Franzén, M.; Ostwald, M.; Berndes, G.; Lakshmi, G.; Ravindranath, N. H. Time-Dependent Life Cycle Assessment of Microalgal Biorefi Nery Co-Products. *Biofuels, Bioprod. Biorefining* **2016**, *6* (3), 246–256. https://doi.org/10.1002/bbb.

(28) Williams, P. J. L. B.; Laurens, L. M. L. Microalgae as Biodiesel & Biomass Feedstocks: Review & Analysis of the Biochemistry, Energetics & Economics. *Energy Environ. Sci.*

683 **2010**, *3* (5), 554–590. https://doi.org/10.1039/b924978h.

684 (29) Franz, A.; Lehr, F.; Posten, C.; Schaub, G. Modeling Microalgae Cultivation Productivities
685 in Different Geographic Locations - Estimation Method for Idealized Photobioreactors.
686 *Biotechnol. J.* **2012**, *7* (4), 546–557. https://doi.org/10.1002/biot.201000379.

687 (30) Araújo, R.; Vázquez Calderón, F.; Sánchez López, J.; Azevedo, I. C.; Bruhn, A.; Fluch, S.;
688 Garcia Tasende, M.; Ghaderiardakani, F.; Ilmjärv, T.; Laurans, M.; Mac Monagail, M.;
689 Mangini, S.; Peteiro, C.; Rebours, C.; Stefansson, T.; Ullmann, J. Current Status of the
690 Algae Production Industry in Europe: An Emerging Sector of the Blue Bioeconomy. *Front.*
691 *Mar. Sci.* **2021**, *7* (January), 1–24. https://doi.org/10.3389/fmars.2020.626389.

692 (31) Tsoy, N.; Steubing, B.; van der Giesen, C.; Guinée, J. Upscaling Methods Used in Ex Ante
693 Life Cycle Assessment of Emerging Technologies: A Review. *Int. J. Life Cycle Assess.*
694 **2020**, *25* (9), 1680–1692. https://doi.org/10.1007/s11367-020-01796-8.

695 (32) Cucurachi, S.; Van Der Giesen, C.; Guinée, J. Ex-Ante LCA of Emerging Technologies.
696 *Procedia CIRP* **2018**, *69* (May), 463–468. https://doi.org/10.1016/j.procir.2017.11.005.

697 (33) Bergerson, J. A.; Brandt, A.; Cresko, J.; Carbajales-Dale, M.; MacLean, H. L.; Matthews,
698 H. S.; McCoy, S.; McManus, M.; Miller, S. A.; Morrow, W. R.; Posen, I. D.; Seager, T.;
699 Skone, T.; Sleep, S. Life Cycle Assessment of Emerging Technologies: Evaluation
700 Techniques at Different Stages of Market and Technical Maturity. *J. Ind. Ecol.* **2020**, *24*
701 (1), 11–25. https://doi.org/10.1111/jiec.12954.

702 (34) Pérez-López, P.; Montazeri, M.; Feijoo, G.; Moreira, M. T.; Eckelman, M. J. Integrating
703 Uncertainties to the Combined Environmental and Economic Assessment of Algal

704 Biorefineries: A Monte Carlo Approach. *Sci. Total Environ.* **2018**, *626*, 762–775.
705 https://doi.org/10.1016/j.scitotenv.2017.12.339.

706 (35) Duran Quintero, C.; Ventura, A.; Lépine, O.; Pruvost, J. Eco-Design of Spirulina Solar
707 Cultivation: Key Aspects to Reduce Environmental Impacts Using Life Cycle Assessment.
708 *J. Clean. Prod.* **2021**, *299*, 126741.
709 https://doi.org/https://doi.org/10.1016/j.jclepro.2021.126741.

710 (36) Tu, Q.; Eckelman, M.; Zimmerman, J. Meta-Analysis and Harmonization of Life Cycle
711 Assessment Studies for Algae Biofuels. *Environ. Sci. Technol.* **2017**, *51* (17), 9419–9432.
712 https://doi.org/10.1021/acs.est.7b01049.

713 (37) Helton, J. C.; Johnson, J. D.; Oberkampf, W. L.; Sallaberry, C. J. Representation of Analysis
714 Results Involving Aleatory and Epistemic Uncertainty. *Int. J. Gen. Syst.* **2010**, *39* (6), 605–
715 646. https://doi.org/10.1080/03081079.2010.486664.

716 (38) Jouannais, P.; Hindersin, S.; Löhn, S.; Pizzol, M. Stochastic LCA Model of Upscaling the
717 Production of Microalgal Compounds. *Environ. Sci. Technol.* **2022**.
718 https://doi.org/10.1021/acs.est.2c00372.

719 (39) Mutel, C. Brightway: An Open Source Framework for Life Cycle Assessment. *J. Open*
720 *Source Softw.* **2017**, *2* (12), 236. https://doi.org/10.21105/joss.00236.

721 (40) Jouannais, P. GitHub repository: PJGilmw/Bioprospected_LCA:
722 Bioprospected_LCA_v1.0.0. **2022**. https://doi.org/10.5281/ZENODO.6789011.

723 (41) 't Lam, G. P.; Vermuë, M. H.; Eppink, M. H. M.; Wijffels, R. H.; van den Berg, C. Multi-
724 Product Microalgae Biorefineries: From Concept Towards Reality. *Trends Biotechnol.*

2018, *36* (2), 216–227. https://doi.org/10.1016/j.tibtech.2017.10.011.

(42) Ruiz, J.; Olivieri, G.; De Vree, J.; Bosma, R.; Willems, P.; Reith, J. H.; Eppink, M. H. M.; Kleinegris, D. M. M.; Wijffels, R. H.; Barbosa, M. J. Towards Industrial Products from Microalgae. *Energy Environ. Sci.* **2016**, *9* (10), 3036–3043. https://doi.org/10.1039/c6ee01493c.

(43) Jahangir, M. H.; Labbafi, S. Optimization of Ground Source Heat Pump System along with Energy Storage Tank Armed with Phase Change Materials to Improve the Microalgae Open Culture System Performance. *J. Energy Storage* **2022**, *51* (April), 104436. https://doi.org/10.1016/j.est.2022.104436.

(44) Schmidt, J. H. Life Cycle Assessment of Five Vegetable Oils. *J. Clean. Prod.* **2015**, *87* (C), 130–138. https://doi.org/10.1016/j.jclepro.2014.10.011.

(45) Huld, T.; Mu, R. A New Solar Radiation Database for Estimating PV Performance in Europe and Africa. **2012**, *86*, 1803–1815. https://doi.org/10.1016/j.solener.2012.03.006.

(46) Metting, F. B. Biodiversity and Application of Microalgae. *J. Ind. Microbiol. Biotechnol.* **1996**, *17* (5–6), 477–489. https://doi.org/10.1007/bf01574779.

(47) Zabed, H. M.; Akter, S.; Yun, J.; Zhang, G.; Zhang, Y.; Qi, X. Biogas from Microalgae: Technologies, Challenges and Opportunities. *Renew. Sustain. Energy Rev.* **2020**, *117* (July 2018), 109503. https://doi.org/10.1016/j.rser.2019.109503.

(48) Hemaiswarya, S.; Raja, R.; Kumar, R. R.; Ganesan, V.; Anbazhagan, C. Microalgae: A Sustainable Feed Source for Aquaculture. *World J. Microbiol. Biotechnol.* **2011**, *27* (8), 1737–1746. https://doi.org/10.1007/s11274-010-0632-z.

746 (49) Skarka, J. Microalgae Biomass Potential in Europe. *TATuP - Zeitschrift für Tech. Theor.*
747 *und Prax.* **2012**, *21* (1), 72–79. https://doi.org/10.14512/tatup.21.1.72.

748 (50) Weidema, B. P.; Ekvall, T.; Heijungs, R. Guidelines for Application of Deepened and
749 Broadened LCA. *Guidel. Appl. Deep. broadened LCA. Deliv. D18 Work Packag. 5 CALCAS*
750 *Proj.* **2009**, No. 037075, 49.

751 (51) Weidema, B. P.; Frees, N.; Nielsen, A.-M. Marginal Production Technologies LCA
752 Methodology. *Int. J. Life Cycle Assess.* **1999**, *4* (1), 48–56.

753 (52) Herman, J.; Usher, W. SALib : Sensitivity Analysis Library in Python (Numpy). Contains
754 Sobol , SALib : An Open-Source Python Library for Sensitivity Analysis. *J. Open Source*
755 *Softw.* **2017**, *2* (9), 97. https://doi.org/10.1016/S0010-1.

756 (53) Pérez-López, P.; de Vree, J. H.; Feijoo, G.; Bosma, R.; Barbosa, M. J.; Moreira, M. T.;
757 Wijffels, R. H.; van Boxtel, A. J. B.; Kleinegris, D. M. M. Comparative Life Cycle
758 Assessment of Real Pilot Reactors for Microalgae Cultivation in Different Seasons. *Appl.*
759 *Energy* **2017**, *205*, 1151–1164. https://doi.org/10.1016/j.apenergy.2017.08.102.

760 (54) Onorato, C.; Rösch, C. Comparative Life Cycle Assessment of Astaxanthin Production with
761 Haematococcus Pluvialis in Different Photobioreactor Technologies. *Algal Res.* **2020**, *50*
762 (March), 102005. https://doi.org/10.1016/j.algal.2020.102005.

763 (55) Frey, H. C. Quantitative Analysis of Uncertainty and Variability in Environmental Policy
764 Making. *AAAS/EPA Environ. Sci. Eng.* **1992**, No. 919, TS-RIS.

765 (56) Michiels, F.; Geeraerd, A. Two - Dimensional Monte Carlo Simulations in LCA : An
766 Innovative Approach to Guide the Choice for the Environmentally Preferable Option. *Int.*

767 *J. Life Cycle Assess.* **2022**, No. 0123456789. https://doi.org/10.1007/s11367-022-02041-0.

768 (57) Hauck, M.; Steinmann, Z. J. N.; Laurenzi, I. J.; Karuppiah, R.; Huijbregts, M. A. J. How to
769 Quantify Uncertainty and Variability in Life Cycle Assessment: The Case of Greenhouse
770 Gas Emissions of Gas Power Generation in the US. *Environ. Res. Lett.* **2014**, *9* (7).
771 https://doi.org/10.1088/1748-9326/9/7/074005.

772 (58) Huijbregts, M. A. J. Application of Uncertainty and Variability in LCA. Part I: A General
773 Framework for the Analysis of Uncertainty and Variability in Life Cycle Assessment. *Int.*
774 *J. Life Cycle Assess.* **1998**, *3* (5), 273–280. https://doi.org/10.1007/BF02979835.

775 (59) Brindhadevi, K.; Mathimani, T.; Rene, E. R.; Shanmugam, S.; Chi, N. T. L.; Pugazhendhi,
776 A. Impact of Cultivation Conditions on the Biomass and Lipid in Microalgae with an
777 Emphasis on Biodiesel. *Fuel* **2021**, *284* (October 2020), 119058.
778 https://doi.org/10.1016/j.fuel.2020.119058.

779 (60) Robert, A.; Fontaine, C.; Veron, S.; Monnet, A. C.; Legrand, M.; Clavel, J.; Chantepie, S.;
780 Couvet, D.; Ducarme, F.; Fontaine, B.; Jiguet, F.; le Viol, I.; Rolland, J.; Sarrazin, F.;
781 Teplitsky, C.; Mouchet, M. Fixism and Conservation Science. *Conserv. Biol.* **2017**, *31* (4),
782 781–788. https://doi.org/10.1111/cobi.12876.

783 (61) Coons, J. E.; Kalb, D. M.; Dale, T.; Marrone, B. L. Getting to Low-Cost Algal Biofuels: A
784 Monograph on Conventional and Cutting-Edge Harvesting and Extraction Technologies.
785 *Algal Res.* **2014**, *6* (PB), 250–270. https://doi.org/10.1016/j.algal.2014.08.005.

786 (62) Eppley, R. W.; Holmes, R. W.; Strickland, J. D. H. Sinking Rates of Marine Phytoplankton
787 Measured with a Fluorometer. *J. Exp. Mar. Bio. Ecol.* **1967**, *1* (2), 191–208.

788 https://doi.org/10.1016/0022-0981(67)90014-7.

789 (63) Najjar, Y. S. H.; Abu-Shamleh, A. Harvesting of Microalgae by Centrifugation for
790 Biodiesel Production: A Review. *Algal Res.* **2020**, *51* (July), 102046.
791 https://doi.org/10.1016/j.algal.2020.102046.

792 (64) Elton, E. J.; Gruber, M. J.; Blake, C. R. Survivor Bias and Mutual Fund Performance. *Rev.*
793 *Financ. Stud.* **1996**, *9* (4), 1097–1120. https://doi.org/10.1093/rfs/9.4.1097.

794 (65) Klein, D. A.; Wu, S. Stress: A Factor to Be Considered in Heterotrophic Microorganism
795 Enumeration from Aquatic Environments. *Appl. Microbiol.* **1974**, *27* (2), 429–431.
796 https://doi.org/10.1128/aem.27.2.429-431.1974.

797 (66) Susilaningsih, D.; Khuzaemah; Rahman, D. Y.; Sekiguchi, H. Screening for Lipid Depositor
798 of Indonesian Microalgae Isolated from Seashore and Peat-Land. *Int. J. Hydrogen Energy*
799 **2014**, *39* (33), 19394–19399. https://doi.org/10.1016/j.ijhydene.2014.08.003.

800 (67) Herrmann, I. T.; Hauschild, M. Z.; Sohn, M. D.; Mckone, T. E. Confronting Uncertainty in
801 Life Cycle Assessment Used for Decision Support: Developing and Proposing a Taxonomy
802 for LCA Studies. *J. Ind. Ecol.* **2014**, *18* (3), 366–379. https://doi.org/10.1111/jiec.12085.

803 (68) Parvatker, A. G.; Tunceroglu, H.; Sherman, J. D.; Coish, P.; Anastas, P.; Zimmerman, J. B.;
804 Eckelman, M. J. Cradle-to-Gate Greenhouse Gas Emissions for Twenty Anesthetic Active
805 Pharmaceutical Ingredients Based on Process Scale-Up and Process Design Calculations.
806 *ACS Sustain. Chem. Eng.* **2019**, *7* (7), 6580–6591.
807 https://doi.org/10.1021/acssuschemeng.8b05473.

808 (69) Mendoza Beltran, A.; Prado, V.; Font Vivanco, D.; Henriksson, P. J. G.; Guinée, J. B.;

809 Heijungs, R. Quantified Uncertainties in Comparative Life Cycle Assessment: What Can
810 Be Concluded? *Environ. Sci. Technol.* **2018**, *52* (4), 2152–2161.
811 https://doi.org/10.1021/acs.est.7b06365.

812 (70) Gotelli, N. J.; McGill, B. J. Null Versus Neutral Models: What's The Difference?
813 *Ecography (Cop.).* **2006**, *29* (5), 793–800.
814 https://doi.org/https://doi.org/10.1111/j.2006.0906-7590.04714.x.

815

816 **Abstract art for Table Of Content**

817

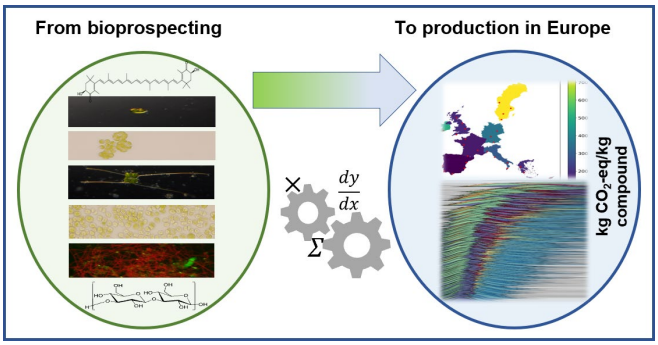

818